ce/papers Proceedings in civil engineering

Ernst & Sohn A Wiley Brand

Check for updates

Full paper

Carbon Footprint of Wire Arc Additively Manufactured Optimized Structural Steel Element

Lidiana Arrè[1] | Emanuele Pagone[2] | Vittoria Laghi[1] | Filomeno Martina[3] | Michele Palermo[1]

Correspondence

Lidiana Arrè
Department of Civil, Chemical, Environmental and Materials Engineering (DICAM) – University of Bologna
Viale del Risorgimento, 2
40136 Bologna
Email: lidiana.arre2@unibo.it

[1] Department of Civil, Chemical, Environmental and Materials Engineering (DICAM) – University of Bologna, Bologna, Italy
[2] Sustainable Manufacturing Systems Centre, School of Aerospace, Transport and Manufacturing, Cranfield University, Cranfield, United Kingdom
[3] School of Management, School of Aerospace, Transport and Manufacturing, Cranfield University, Cranfield, United Kingdom

Abstract

Metal Additive Manufacturing (AM), and particularly Wire Arc Additive Manufacturing (WAAM), opens new opportunities for steel structures by enabling efficient, reliable, and material-saving solutions with reduced environmental impact. The AEC sector is starting to adopt WAAM for full-scale structural elements, benefiting from its design freedom. However, tailored design approaches are needed to fully harness its potential and realize geometries unachievable with conventional methods. This study evaluates the environmental performance of a novel steel structural element featuring a Tubular Sandwich Section (TSS), fabricated using WAAM. The TSS, which defines the section of the structural element, consists of inner and outer cylinders connected by internal spokes, providing improved radial strength and better alignment with structural requirements. Its performance is compared to that of a conventional Circular Hollow Section (CHS), manufactured through cold forming with equivalent diameter and radial capacity. A cradle-to-gate analysis shows that WAAM enables a lighter and more sustainable alternative, highlighting its promise in reducing the carbon footprint of the construction sector.

Keywords

design for additive manufacturing, structural optimization, 3D printing, wire arc additive manufacturing, carbon footprint, sustainability

1 Introduction

The construction sector plays a crucial role in economic development but is also among the most environmentally intensive industries, contributing to 37% of global emissions related to material production [1,2]. A major share of this impact comes from the steel industry, responsible for approximately 3.6 Gt of CO_2 emissions in 2019, over 8% of global energy use [3]. Although energy efficiency has improved, current progress remains insufficient to meet Net Zero Emissions targets by 2050 [4].

In response, sustainable manufacturing practices are gaining importance. Metal Additive Manufacturing (AM), and in particular Wire Arc Additive Manufacturing (WAAM), has emerged as a promising alternative to conventional production processes, enabling significant improvements in material efficiency and geometric freedom [5]. WAAM uses an electric arc to melt wire feedstock, depositing material with deposition rates up to 9.5 kg/h, with less material waste, near-total material utilization, and good quality of the outcomes in terms of geometrical and mechanical features [6–9].

In structural engineering, WAAM allows for the fabrication of complex and performance-optimized geometries that are difficult to achieve using conventional methods [10]. In particular, in the offshore engineering sector, steel structures mainly subjected to high radial pressure, such as tubular members for offshore jackets, are conventionally designed and fabricated as Circular Hollow Section (CHS), due to the advantages in terms of high strength-to-weight ratio and good hydrodynamic performance derived from by-symmetrical cross-sectional shape. On the other hand, buckling failure may occur at high D/t ratios, limiting their adoption.

The presented WAAM Tubular Sandwich Section (TSS) represents a novel steel profile, which offers greater freedom in geometrical configuration, enabling the design of optimized shapes characterized by enhanced buckling resistance and material savings. Prototypes were manufactured as a proof of concept and presented in [11], using a

© 2026 The Author(s). Published by Ernst & Sohn GmbH.

https://doi.org/10.1002/cepa.70161

This is an open access article under the terms of the Creative Commons Attribution License, which permits use, distribution and reproduction in any medium, provided the original work is properly cited.

layer-by-layer deposition strategy in which successive layers of molten metal are deposited on top of each other.

This study applies a cradle-to-gate Life Cycle Assessment (LCA) to compare the carbon footprint of two approaches: WAAM-based manufacturing of a TSS structural element and cold-formed manufacturing of a CHS structural element. The objective is to quantify the carbon footprint and assess WAAM's potential as a sustainable manufacturing method for future structural applications.

2 TSS design

The geometrical configuration of a TSS structural element has been introduced in [11], consisting of two cylindrical walls connected by a number of spokes of equal length forming triangular shapes, as shown in Figure 1, in which the main geometrical parameters are reported. The number of geometrical parameters provides greater design freedom.

The TSS configuration has been designed to enhance structural performance under radial compression by integrating spokes that connect the inner and outer cylinders. The outer cylinder, which is directly exposed to radial pressure, has been designed with greater thickness. On the contrary, the inner cylinder and spokes, whose primary function is to restrain the outer cylinder by reducing the free buckling length (arch between consecutive spokes), have been designed with a reduced thickness compared to the outer cylinder.

On the other hand, the CHS structural element is characterized by a cylindrical wall and fewer geometrical parameters, such as external diameter and thickness (Fig.2).

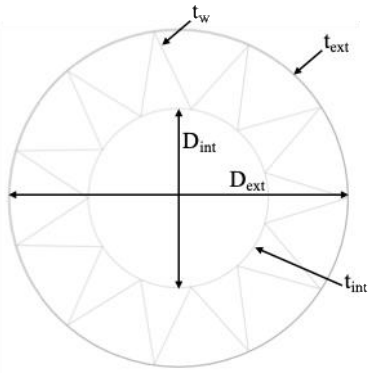

Figure 1 Geometrical configuration and parameters of TSS. Adapted from [11].

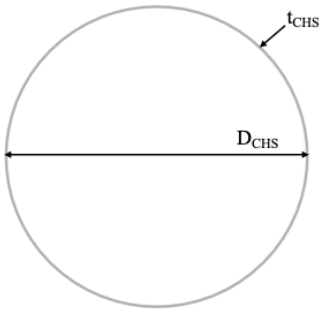

Figure 2 Geometrical configuration and parameters of CHS. Adapted from [11].

3 Methodology

3.1 Functional unit and system boundaries

This study evaluates the carbon footprint of the two alternative tubular steel elements for structural applications, each manufactured with a different production process, enabling a consistent comparison between conventional cold-formed and WAAM. The two structural elements under investigation are characterized by different sections: (i) cold-formed Circular Hollow Section (CHS), and (ii) Tubular Sandwich Section (TSS) produced using WAAM. Mass production is assumed for both configurations.

The functional unit is defined as a tubular steel element with a length of 2 meters and an external diameter of 1.4 m, designed to meet the same structural requirements in terms of radial pressure capacity. This definition ensures functional equivalence between the two geometries, enabling a meaningful comparative LCA.

The CHS has a nominal thickness of 12.8 mm and represents a standard industrial component widely used in offshore and infrastructure applications (Fig.2). The TSS configuration evaluated here includes an external wall with 6 mm thickness, an internal wall with 2 mm thickness, and 22 spokes of 2 mm thickness (Fig.1). The geometry was developed using a blended design methodology combining structural design, generative algorithms and WAAM-specific manufacturing constraints [12,13]. Although the TSS geometry analyzed in this study differs from the one physically prototyped in [11], the carbon footprint assessment is based on the same manufacturing process parameters, which were experimentally validated in the earlier prototype.

The system boundaries are defined according to a cradle-to-gate approach, encompassing all stages from raw material extraction to the completion of the structural element, including steel production and transformation processes. For the CHS, the system includes raw material extraction, transportation to the steel production facility, cold-forming and welding to manufacture the final element (Fig.3). Figure 4 shows the system boundaries for the WAAM TSS, encompassing the production of welding wire and shielding gas, their transport and use in the manufacturing process. The welding wire production includes raw material extraction, hot rolling to produce wire rods, transportation to the wire drawing facility to obtain the final welding wire. The shielding gas production involves the cryogenic separation of argon and the capture of carbon dioxide as by-product.

WAAM-specific steps, including energy use and material losses during deposition, are discussed in detail in the Section 3.2.

25097075, 2025, 6, Downloaded from https://onlinelibrary.wiley.com/doi/10.1002/cepa.70161 by Area Sistemi Dipart & Doc, Wiley Online Library on [25/02/2026]. See the Terms and Conditions (https://onlinelibrary.wiley.com/terms-and-conditions) on Wiley Online Library for rules of use; OA articles are governed by the applicable Creative Commons License

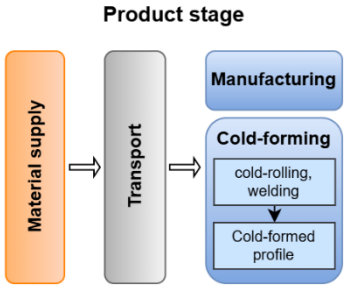

Figure 3 System boundaries of cold-formed CHS structural element.

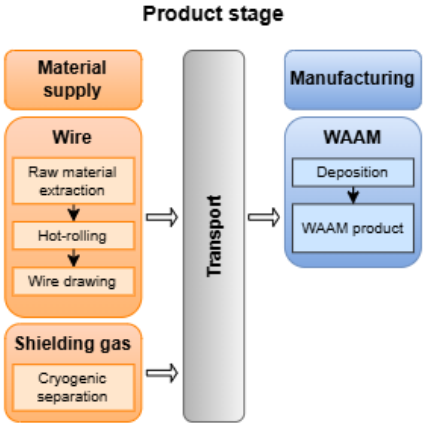

Figure 4 System boundaries of TSS WAAM structural element.

3.2 Inventory analysis

The cradle-to-gate analysis is conducted differently for the two structural elements. The Global Warming Potential (GWP), expressed in terms of kilograms of CO_2-equivalent ($kgCO_2eq$), is adopted to quantify the carbon footprint of each production route.

Information on the cold-formed CHS was obtained from Environmental Product Declarations (EPDs) specific to CHS production, available through the Building Transparency database [14]. These EPDs report GWP values based on the aggregated inputs and outputs involved in the manufacturing of CHS structural elements.

In contrast, no EPDs are currently available for WAAM-produced elements. Therefore, a process-based approach was adopted, considering the direct inputs to the WAAM process, including welding wire, shielding gas and electricity consumed by welding and robotic movement, as well as outputs, such as the WAAM TSS element and associated metal material losses, detailed in Section 3.2.2.

3.2.1 Cold-formed CHS structural element

The production of the CHS steel structural element through cold-forming involves raw material sourcing, steel coil processing and shaping into circular profiles. The process includes slitting, cold-rolling and welding steps, accounting for energy and material inputs.

For the carbon footprint assessment, data were sourced from EPDs, considering the cradle-to-gate approach and including emissions from raw material extraction to the final manufacturing stage. To reflect geographic variability, EPDs from European and Asian producers were considered, referring to the available ones, and an average value was used for comparison with the WAAM TSS production.

3.2.2 WAAM TSS structural element

This study evaluates the carbon footprint of producing the WAAM TSS structural element at AITIIP Centro Tecnológico (Zaragoza, Spain) [11]. The set-up included Fronius TPS 400i power source with WF 60i Robacta CMT torch, Yaskawa GP50 robotic arm and SanArc C8 shielding gas provided by Nippon Gases. The welding wire used was ER70S-6 Ultramag of 1.2 mm, supplied by Lincoln Electric [15–19].

The production chain involves multiple stages. The main process inputs are electricity, welding wire and shielding gas, outputs include the manufactured TSS element, material losses (trimming scrap, welding spatter, and cut wire) and emissions associated with energy use and transportation. The subplate used during deposition is not included in the system boundaries, as it is reused across multiple production cycles.

The initial steps include the production of welding wire and shielding gas, as key inputs for the WAAM process. Wire production comprises raw material extraction, hot rolling to obtain steel wire rods, and subsequent wire drawing to achieve the final welding wire diameter (typically ranging between 0.8 mm and 1.2 mm). Carbon footprint data for welding wire production were sourced from technical data sheets and manufacturer sustainability reports [18,19]. In parallel, shielding gas is produced by mixing 92% argon, obtained through cryogenic air separation, and 8% carbon dioxide, typically recovered as a by-product from other industrial processes, followed by purification and compression into refillable steel cylinders for distribution. Carbon footprint data for shielding gas were obtained using the ecoinvent database [20].

Both welding wire and shielding gas are transported to the WAAM facility, where the additive deposition takes place. Transportation emissions were estimated considering typical transport modes (e.g. truck > 32t EURO4 and rail), based on distances from production sites (Germany and Spain for welding wire and shielding gas, respectively) to the WAAM facility in Spain, using emission factors sourced from Granta EduPack 2023 R2 [21].

Energy consumption for WAAM includes both welding and robotic movement, with values estimated from equipment specifications and process parameters. A European average electricity emission factor of 0.17 $kgCO_2eq/kWh$ was used, reflecting a grid mix of 39% fossil fuels, 39% renewables, and 22% nuclear [22].

Material losses across the production chain were modeled using utilization rates: 0.95 for hot rolling, based on the average value reported in Granta EduPack 2023 R2 [21], 0.90 for wire drawing, and 0.99 for WAAM, to account for material losses [3]. As a result, 1.18 kg of steel is required to produce 1 kg of the WAAM TSS structural element.

25097075, 2025, 6, Downloaded from https://onlinelibrary.wiley.com/doi/10.1002/cepa.70161 by Area Sistemi Dipart & Doc, Wiley Online Library on [25/02/2026]. See the Terms and Conditions (https://onlinelibrary.wiley.com/terms-and-conditions) on Wiley Online Library for rules of use; OA articles are governed by the applicable Creative Commons License

4 Results

The carbon footprint associated with the production of the cold-formed CHS and WAAM TSS structural elements were quantified and illustrated in Figure 5. The average GWP for CHS production was determined by analyzing data from nine European and Asian producers through available EPDs, to account for production variability across different continents, resulting in an average GWP of 2.46 $kgCO_2eq$ per kg of CHS. In contrast, the WAAM TSS production exhibits a higher impact per unit of mass, with a GWP of 2.59 $kgCO_2eq$ per kg of WAAM printed material. This represents an approximate 5.3% increase in GWP per kg compared to CHS. However, due to its high structural efficiency with an optimized configuration, the TSS significantly reduces total mass. Specifically, it weighs approximately 17% less than the CHS counterpart while ensuring equivalent structural performance. As a result, the WAAM TSS exhibits a lower overall carbon footprint, amounting to a 13% reduction in total CO_2-equivalent emissions compared to the CHS (Fig.5).

The breakdown of carbon emission sources highlights that the most impactful stages in the WAAM TSS production are material supply with 68%, accounting for welding wire and shielding gas, and the WAAM manufacturing itself with 27%, with the remaining contribution provided by transport (Fig. 6). The wire's impact represents more than half of the material supply's impact and is primarily linked to upstream steel production, which has been assumed to reflect a 50% allocation to each route (such as blast furnace and electric arc furnace) based on the CO2-emission targets stated in the company report [19].

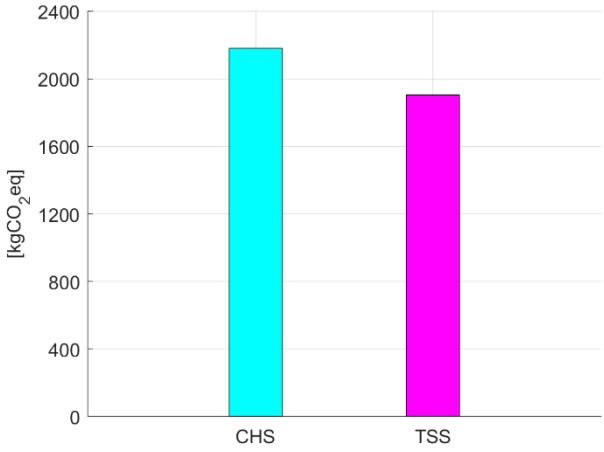

Figure 5 Carbon footprint of cold-formed CHS and WAAM TSS structural elements.

5 Conclusion

This study presents the comparative LCA conducted on the novel TSS structural element manufactured using WAAM and conventional cold-formed CHS structural element. WAAM offers advantages in manufacturing highly efficient structural elements with complex cross-sections that are either unfeasible or extremely labor-intensive using conventional methods. This enables the development of novel structural configurations with greater design freedom, allowing for significant material savings. Therefore, despite the higher GWP per kg of WAAM printed material, the carbon footprint of the WAAM TSS structural element is lower compared to the cold-formed CHS counterpart, characterized by the same structural performance in terms of radial compression. As a consequence, WAAM is assessed as a potential sustainable manufacturing method for future structural applications.

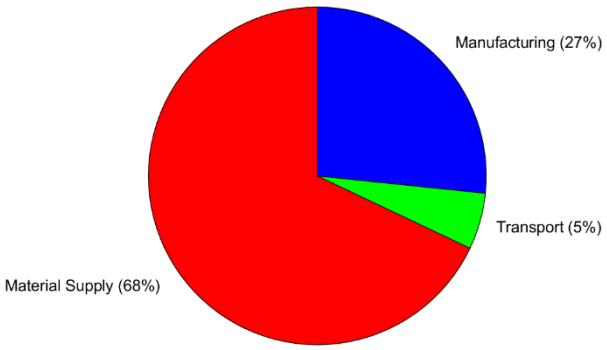

Figure 6 Pie chart of the carbon emission contributions of WAAM TSS structural element.

The highest carbon emission source in the WAAM TSS production is associated with the welding wire production, which is responsible for more than half the material supply's impact. In particular, the steel production remains partially dependent on conventional blast furnace routes. A transition toward fully electric arc furnace (EAF) production, coupled with a renewable energy supply, could significantly reduce emissions at this stage.

Similarly, the energy required for WAAM, specifically for welding and robotic movement, accounts for a substantial portion of the total impact. Since these operations are electricity-intensive, adopting a cleaner, more renewable energy mix would result in a meaningful decrease in emissions. This underlines the importance of energy source decarbonization for both upstream material processing and WAAM manufacturing operations.

Future studies will aim to expand the dataset, particularly by including a broader range of welding wire producers. Currently, data availability for wires with diameters between 0.8 mm and 1.2 mm is limited, yet this component represents the most impactful contribution to the carbon footprint of the WAAM TSS structural element. Additional shielding gas producers and a wider range of gas mixture compositions will also be considered to generalize the carbon footprint assessment beyond the specific case of the 92% argon and 8% carbon dioxide mixture.

Further refinements will address the electricity consumption associated with robotic movement. The current estimation is based on the rated power reported in technical datasheets, which may overestimate actual electricity consumption during WAAM operations, as it does not reflect real operating conditions. Future analyses will focus on

25097075, 2025, 6, Downloaded from https://onlinelibrary.wiley.com/doi/10.1002/cepa.70161 by Area Sistemi Dipart & Doc, Wiley Online Library on [25/02/2026]. See the Terms and Conditions (https://onlinelibrary.wiley.com/terms-and-conditions) on Wiley Online Library for rules of use; OA articles are governed by the applicable Creative Commons License

measuring the actual energy use during WAAM operations to provide a more accurate and representative carbon footprint assessment.

The extended methodological approach will be validated through additional case studies to confirm its applicability and robustness across different production scenarios.

6 Acknowledgements

The authors acknowledge AITIIP Centro Tecnológico in Zaragoza (Spain) for fabricating the WAAM TSS and providing technical data. The authors also gratefully acknowledge Lincoln Electric for sharing information on wire production.

References

[1] UNEP (2025) Nairobi 2023 [online]. Nairobi: UNEP. https://www.unep.org/resources/report/building-materials-and-climate-constructing-new-future.

[2] Kokare, S.; Oliveira, J. P.; Godina, R. (2023) *A LCA and LCC analysis of pure subtractive manufacturing, wire arc additive manufacturing, and selective laser melting approaches*. Journal of Manufacturing Processes 101, p. 67–85. https://doi.org/10.1016/J.JMAPRO.2023.05.102.

[3] Shah, I. H.; Hadjipantelis, N.; Walter, L. et al. (2023) *Environmental life cycle assessment of wire arc additively manufactured steel structural components.* Journal of Cleaner Production 389. https://doi.org/10.1016/J.JCLEPRO.2023.136071.

[4] IEA (n.d.) International Energy Agency website [online]. https://www.iea.org.

[5] Gardner, L. (2023) *Metal additive manufacturing in structural engineering – review, advances, opportunities and outlook*. Structures 47, p. 2178–2193. https://doi.org/10.1016/J.ISTRUC.2022.12.039.

[6] Martina, F.; Ding, J.; Williams, S. et al. (2019) *Tandem metal inert gas process for high productivity wire arc additive manufacturing in stainless steel.* Additive Manufacturing 25, p. 545–550. https://doi.org/10.1016/J.ADDMA.2018.11.022.

[7] Silvestru, V. A.; Ariza, I.; Taras, A. (2023) *Structural behaviour of point-by-point wire arc additively manufactured steel bars under compressive loading.* Journal of Constructional Steel Research 207. https://doi.org/10.1016/j.jcsr.2023.107982.

[8] Laghi, V.; Arrè, L.; Tonelli, L. et al. (2023) *Mechanical and microstructural features of wire-and-arc additively manufactured carbon steel thick plates*. International Journal of Advanced Manufacturing Technology 127, p. 1391–1405. https://doi.org/10.1007/S00170-023-11538-3/FIGURES/11.

[9] Kokare, S.; Shen, J.; Fonseca, P. P. et al. (2024) *Wire arc additive manufacturing of a high-strength low-alloy steel part: environmental impacts, costs, and mechanical properties*. International Journal of Advanced Manufacturing Technology 134, p. 453–475. https://doi.org/10.1007/S00170-024-14144-Z/TABLES/7.

[10] Baqershahi, M. H.; Ayas, C.; Ghafoori, E. (2024) *Design optimisation for hybrid metal additive manufacturing for sustainable construction*. Engineering Structures 301, 117355. https://doi.org/10.1016/J.ENGSTRUCT.2023.117355.

[11] Arrè, L.; Laghi, V.; Paola, A. M. et al. (2024*) Tubular sandwich cross-sections fabricated with Wire Arc Additive Manufacturing for jumbo structural members.* Structures 67, 106689. https://doi.org/10.1016/J.ISTRUC.2024.106689.

[12] Laghi, V.; Palermo, M.; Bruggi, M. et al. (2022) *Blended structural optimization for wire-and-arc additively manufactured beams*. Progress in Additive Manufacturing. https://doi.org/10.1007/s40964-022-00335-1.

[13] Oliveira, J. P.; Gouveia, F. M.; Santos, T. G. (2022) *Micro wire and arc additive manufacturing (μ-WAAM)*. Additive Manufacturing Letters 2, 100032. https://doi.org/10.1016/J.ADDLET.2022.100032.

[14] Building Transparency (n.d.) Embodied Carbon in Construction Calculator (EC3) [online]. https://buildingtransparency.org/ec3.

[15] Fronius (n.d.) Fronius International GmbH [online]. https://www.fronius.com/enhttps://.

[16] Yaskawa (n.d.) Yaskawa Europe [online]. www.yaskawa.eu.com.

[17] Nippon Gases (n.d.) Nippon Gases Europe [online]. https://nippongases.com/gb-en.

[18] Lincoln Electric (n.d.) Lincoln Electric Holdings, Inc. [online]. https://www.lincolnelectric.com/en.

[19] Saarstahl (n.d.) Saarstahl AG [online]. https://en.saarstahl.com.

[20] Ecoinvent (n.d.) ecoinvent - Data with purpose [online]. https://ecoinvent.org/ (accessed April 10, 2025).

[21] Ansys (n.d.) Granta EduPack [software]. https://www.ansys.com/products/materials/granta-edupack.

[22] Ritchie, H.; Rosado, P. (2020) Electricity Mix. Our World in Data [online]. https://ourworldindata.org/electricity-mix

25097075, 2025, 6, Downloaded from https://onlinelibrary.wiley.com/doi/10.1002/cepa.70161 by Area Sistemi Dipart & Doc, Wiley Online Library on [25/02/2026]. See the Terms and Conditions (https://onlinelibrary.wiley.com/terms-and-conditions) on Wiley Online Library for rules of use; OA articles are governed by the applicable Creative Commons License